JMEPEG (1992) 1: 615-624

Effects of Heat Treatment on the Mechanical Properties of SiC*p*/6061 Al Composite

D. Aidun, P. Martin, and J. Sun

Metal-matrix composites have been receiving considerable attention as light-weight materials for use in many advanced technology applications. Silicon carbide (SiC) particles and whiskers have several advantages over other discontinuous reinforcements. Studies have shown that heat treatment can change the mechanical properties of metal-matrix composites.

Modified heat treatments were developed for SiC*p*/6061 Al composites through a series of heat treatment with varied solution temperatures and aging time. Mechanical tests were conducted to determine the mechanical properties of the composites in three conditions; as-received, annealed, and heat treated. The modified heat treatments resulted in increases in the yield strength of up to 12% over the manufacturer's reported yield strength for the standard T6 heat treatment. The trends which occur during heat treatment of SiC*p*/6061 Al are simular to those which occur during heat treatment of aluminum alloys. In addition, the relationship between the mechanical properties and the heat treatment parameters was documented. Throughout this study, the values of elastic modules were rather erratic compared to the strength values. Scanning Electron Microscope fractographic analysis revealed various fracture initiation sites, such as particle clusters and iron inclusions.

1. Introduction

IN recent years, metal-matrix composites (MMC) have received considerable attention as lightweight materials for use in many advanced technology applications. Metal-matrix composites are produced in various forms, including continuous and discontinuous fiber-reinforced composites. Discontinuous fiber composites possess both high specific strength and isotropic properties. Their isotropy, low density, and wear resistance make them desirable for piston, cylinder, and connecting rod materials in the automotive industry. Other applications exist in the aircraft and spacecraft industries. For example, discontinuous fiber composites presently are used in the outer skin and structural ribs in the tail sections of advanced fighters. [1-4]

Metal-matrix composites are defined as materials containing reinforcements in a continuous metal matrix. These reinforcements may include any combination of fibers, wires, single-crystal whiskers, polycrystalline flakes, and nonmetallic particles.[4,5] Particles have low aspect ratios and are usually less expensive than whiskers or fibers. The strengthening mechanism of particles is similar to that of dispersion-strengthened alloys, because particles in the matrix prevent the motion of dislocations.[6,7]

Silicon carbide (SiC) particles and whiskers have several advantages over other discontinuous reinforcements made from alumina, graphite, and boron. For example, SiC is less expensive than other reinforcements, possesses excellent thermal conductivity and corrosion resistance, and has comparatively high machinability and workability.[7] Reinforced SiC particulates (SiC*p*)/aluminum and metal-matrix composites have demonstrated improved mechanical properties over wrought aluminum alloys. These properties include higher elastic moduli and yield strengths, improved creep strengths, and low thermal expansions. In addition, they can be fabricated using many standard manufacturing processes. However, their ductility and fracture toughness are significantly lower than those of wrought alloys.[8]

Most of the matrices in metal-matrix composites are common alloys that are used because of their low cost and/or availability. The mechanical properties of these alloys strongly depend on heat treatment. Studies have shown that heat treatment can also increase the mechanical properties of metal-matrix composites, especially those with discontinuous reinforcements.[3,8-11] The increased matrix yield strength allows for more effective load transfer from the matrix to the reinforcement.[9] Despite these findings, heat treatment of

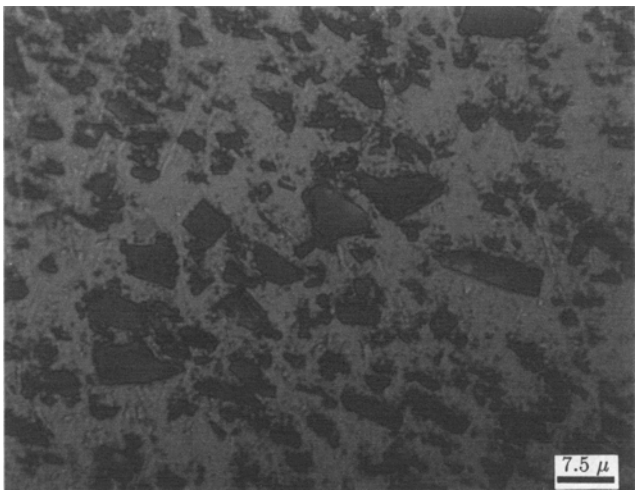

Fig. 1 Microstructure of a SiC*p*/6061 aluminum sample.

D. Aidun (Associate Professor); **P. Martin** (currently with Pratt & Whitney Aircraft Co.); and **J. Sun** (Graduate Student), Mechanical and Aeronautical Engineering Department, Clarkson University, Potsdam, New York.

composites has received little attention. Often, standard heat treatments for the wrought matrix alloys are specified for the composites. However, standard heat treatments do not account for powder metallurgy-induced inhomogeneities, thermal exposure during composite fabrication, the effect of the reinforcement on the strengthening mechanisms of the alloy, or the effect of the heat treatment on the reinforcement. Because of the high cost of composite materials, it is important that optimal mechanical properties are obtained for many advanced technology applications. One way of improving the mechanical properties of composites is through specialized heat treatment techniques.

2. Experimental Procedures

The metal-matrix composite that was investigated was a silicon carbide particle (25 vol%) reinforced 6061 aluminum material (SiC*p*/6061 aluminum), which was produced by powder metallurgy and rolled into sheet form (50 by 35 by 0.1 cm). The microstructure of the composite is shown in Fig. 1. The manufacturer recommended annealing the composite and performing a T6 heat treatment. The annealing cycle is as follows:

- Heat the material to 371 °C and hold for 2 hr
- Cool to 204 °C at 28 °C/hr
- Cool to room temperature (cooling rate is unimportant)

The T6 heat treatment involves (1) heating the material to 530 °C, (2) water quenching to room temperature, and (3) aging the material at 160 °C for 18 hr. The reported mechanical properties of T6 heat treated composite are:

Young's modulus	114 GPa
Yield strength	413 MPa
Ultimate tensile strength	496 MPa
Ductility	4.2%

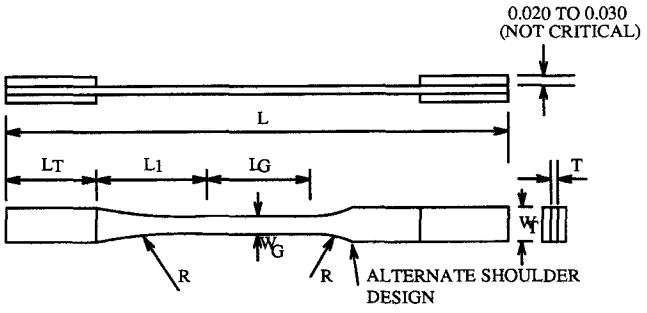

Design	L (mm)	L_T (mm)	L_1 (mm)	L_G (mm)	W_G (mm)	R (mm)
A	127	25	25	25	6.4	25
B	127	25	25	25	9.5	25
C	127	25	-	76	12.7	-
D	127	25	-	51	9.5	-
E	76	19	6.4	25	6.4	12.7
F	76	25	-	25	12.7	-
NS	76	25	-	25	9.5	-

Fig. 2 ASME Standard D 3552-77-C sample design.

The as-received materials were annealed and were cut using a diamond saw. For tension test samples of these materials, ASTM Standard D 3552-77-C[12] was chosen for the sample configuration. A schematic is shown in Fig. 2. Because a large number of tests was necessary, a smaller, nonstandard (NS) sample configuration was adopted.

For the initial tests, eight as-received samples were cut from the composite sheet to document the as-received mechanical properties. Four samples were cut in the transverse direction and four in the longitudinal direction. Next, the composite sheet was annealed as recommended by the manufacturer. After the material was annealed, samples were cut from the sheet, and the sample edges were polished. A series of tension tests showed that edge polishing had no significant effect on tensile strength. Therefore, the remaining tension test samples were used as cut.

For heat treatment, the samples were first placed in a fused quartz ampule, which was attached to the vacuum system using a compression fitting. Next, the air was evacuated and the desired atmosphere induced. The furnace was ramped up to the solution temperature in approximately 15 min. After the desired solution time had passed, the ampule pressure was equalized, the compression fitting released, the furnace opened, and the samples quenched in room-temperature water. Following the solution treatment, the samples were aged as follows:

- Raise the furnace temperature to 160 °C in 30 min.
- Hold that temperature for the required aging time.
- Cool to room temperature.

After aging, the samples were subjected to tensile load on an Instron machine using a stroke rate of 0.5 mm/min.

Fracture surfaces of samples were examined using a scanning electron microscope (SEM). To prepare SEM samples, fractured tensile specimens were cut approximately 1/2 in. from the fracture surface using a silicon carbide cut-off saw.

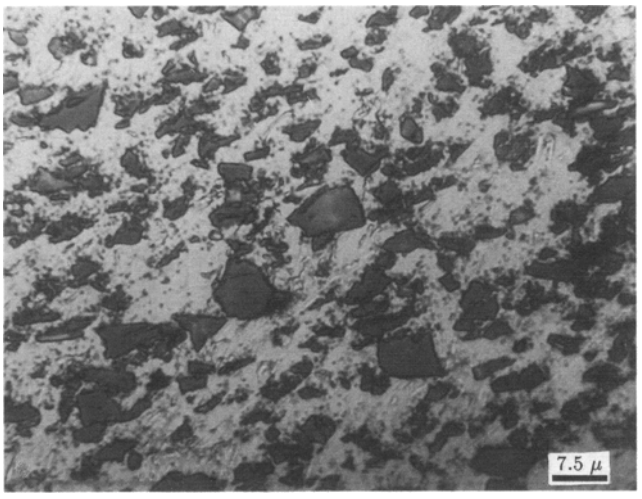

Fig. 3 Micrograph of a polished SiC*p*/6061 aluminum section.

These samples were cleaned in an ultrasonic cleaner using first acetone, then methanol, and finally trichloromethane. The samples were attached to aluminum sample bases with a conducting adhesive containing silver. When the adhesive cured, the samples were ready for SEM and energy-dispersive spectroscopy (EDS) analysis.

3. Results and Discussion

Optical microscopy was performed on the SiC*p*/6061 aluminum composite. A micrograph of the polished cross section of a SiC*p*/6061 aluminum sample is presented in Fig. 3. The SiC particle size varies significantly, which was characteristic of the material.

In the sample, the particles were oriented slightly in the horizontal direction, which corresponds to the longitudinal direction of the sample. This orientation was caused by rolling during manufacturing. The average aspect ratio of the particles in the longitudinal direction was 1.6, with a standard deviation of 0.16. The area percent of SiC particles in this section of the sample was 31%, compared to an overall particle volume percent of 25%. The range of particle ferret diameters was 1 to 15 μm, with the majority of the particle ferret diameters between 1 to 4 μm.

Mechanical tests were conducted to determine the mechanical properties of the composite in three conditions—as-received, annealed, and heat treated. The as-received material had a 0.2% offset yield point of 172 MPa, an ultimate tensile strength of 276 MPa, and an elastic modulus of 90 GPa. These values matched those reported by the manufacturer.[13] For the annealed composite, both the transverse and longitudinal samples had an ultimate tensile strength of 241 MPa, compared to 124 MPa for annealed 6061 aluminum. No significant difference wasobserved between the longitudinal and transverse properties of the as-received or annealed SiC*p*/6061 aluminum samples, as was documented in previous studies.[14,15]

SiC*p*/6061 aluminum is manufactured by hot pressing at temperatures above the solidus temperature of the matrix. Microsegregation due to partial melting of the matrix material may result. In addition, voids and other inhomogeneities may be produced during fabrication by powder metallurgy. In the previous study by Skibo,[9] longer solution times at higher solution temperatures were used to homogenize the matrix material of discontinuous SiC/2024 aluminum composites. The modified solution heat treatment included a 17 °C increase in temperature and an increase in solution time to 72 hr. This solution treatment resulted in mechanical properties that were significantly higher than those of standard T7 heat treated samples.

Prolonged time at the increased temperature during the solution treatment did not increase the mechanical properties of SiC*p*/6061 aluminum, as was reported for SiC/2024 aluminum in the Skibo study. This result could be attributed to several factors. First, the SiC/2024 aluminum composite used by Skibo was not rolled during fabrication, as was the SiC*p*/6061 aluminum composite used in this investigation. Rolling has been shown to increase the mechanical properties of SiC/6061 aluminum by improving metal-to-metal bonding and thus homogenizing the matrix material.[13] Second, Skibo used a solution temperature of 510 °C, which was above the lower bound (502 °C) of the melting temperature range of 2024 aluminum. This heat treatment, although helping to homogenize the matrix, may have led to microsegregation. Third, various other heat treatment parameters were changed in the modified heat treatment used by Skibo, including solution temperature, aging time, and aging temperature. Because so many parameters were changed, it was difficult to relate the results of the modified heat treatment to those of the standard heat treatment. Changes in parameters other than solution time may have partially accounted for the increased mechanical properties.

To determine which heat treatment parameters most affected the mechanical properties of the aluminum composite, samples were subjected to various solution temperatures, solution times, aging temperatures, and aging times.

Due to results reported in previous studies of discontinuous SiC/aluminum, it was anticipated that increased solution temperatures would be required to obtain the best mechanical properties of the SiC*p*/6061 aluminum composite. In previous studies, composite matrices did not reach expected hardness levels during standard heat treatments.[9] This phenomenon may be related to the presence of the SiC particles. Strain fields around the particles are caused by the differential thermal expansions of the particles and the matrix during quenching. Therefore, SiC particles act as sites for nucleation of precipitates during aging. Many of the precipitates in a composite may form at the edges of particles. Thus, the effective particle size would increase, but matrix-rich zones would contain fewer precipitates than expected. At higher solution temperatures, however, the greater degree of supersaturation might cause more precipitates to form in the matrix-rich zones of the composites, as opposed to on the particle edges. Under these conditions, the matrix hardness could reach the predicted hardness of 6061 aluminum in the T6 condition. For this reason, solution temperatures at or above the recommended temperature of 530 °C were examined during this study. Although increased solution temperatures would result in larger grain sizes in unreinforced aluminum alloys, the particles in SiC*p*/6061 aluminum would inhibit extensive grain growth.

Throughout the heat treatment study, the values of the elastic modulus were rather erratic compared to the strength values. In addition, no trends were observed between the elastic modulus and the heat treatment parameters or strength. This lack of correlation is not surprising, because the elastic modulus is a material property and is generally not dependent on heat treatment. The average value of the elastic modulus for all the samples was 105.4 GPa, with a standard deviation of 15.8 GPa. The value of the elastic modulus reported by the manufacturer was 114.0 GPa. The range of the recorded elastic modulus values may have been due to the two phases in the composite. For this reason, deformation would not necessarily occur uniformly throughout the sample. In addition, varying particle sizes and volume fractions were observed during the microstructural evaluation. If the volume percent reinforcement varied from sample to sample, the elastic modulus would be affected.

It is interesting to note that the value of the elastic modulus reported for this material is at the theoretical limit. The Tsai-Halpin model predicts an elastic modulus of 110 GPa for randomly oriented 25 vol% SiC/aluminum composites with a

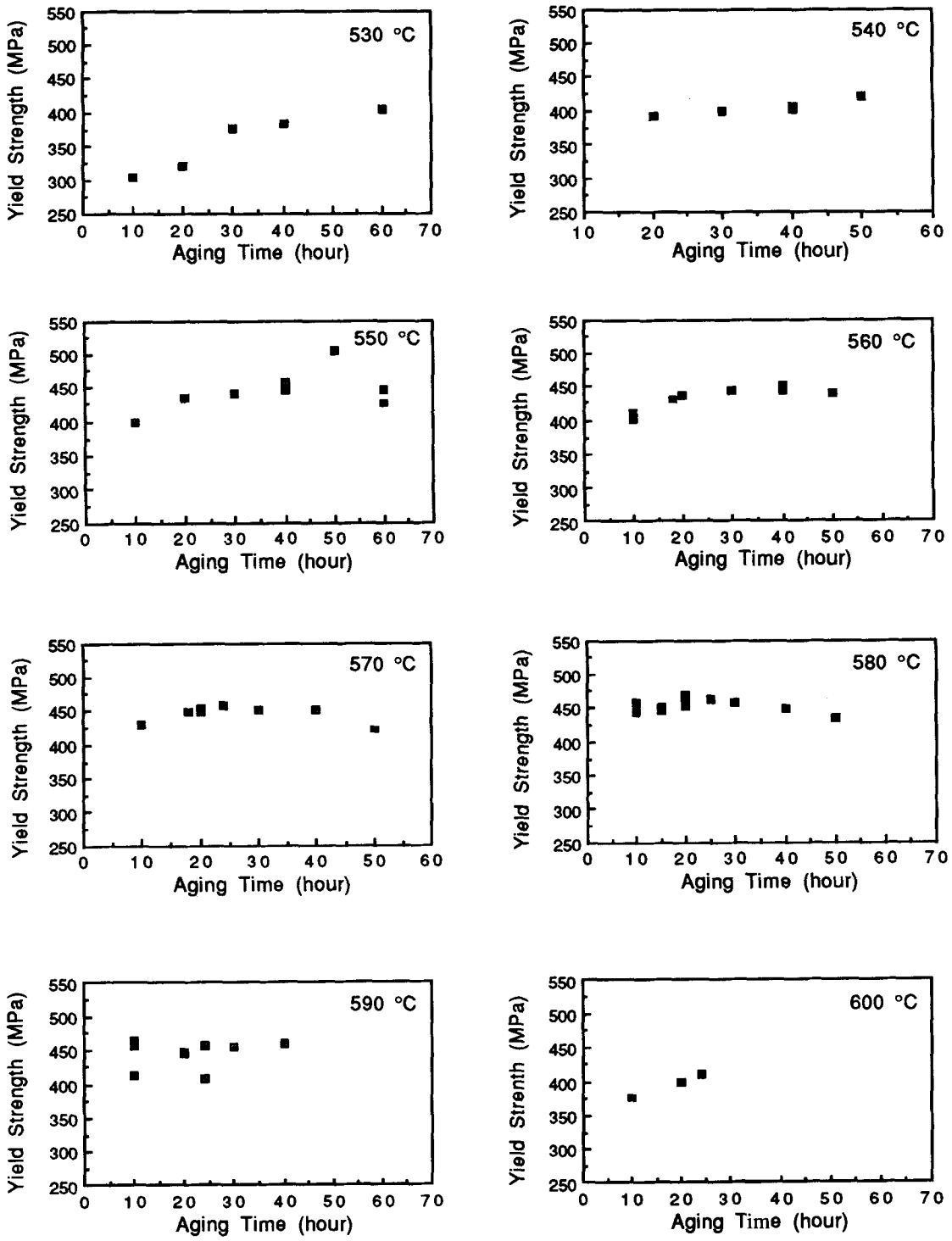

Fig. 4 Yield strength versus aging time (solution temperature 530 to 600 °C).

particle aspect ratio of 1.6. For an oriented composite, the predicted value of the elastic modulus in the longitudinal direction is 117 GPa. Reaching the theoretical limit for the elastic modulus of particle composites has been reported in other studies.[7,9] The increase in the elastic modulus of SiC*p*/aluminum composites over their matrix material is due to a combination of the particle and matrix moduli, which is determined by the volume fraction and orientation of the particles. Thus, in accordance with the Tsai-Halpin model, the full potential of the elastic modulus of many discontinuous reinforced composites has been reached.

During the heat treatment study, yield strength was used to gage the effectiveness of the heat treatment performed on each sample. This choice was based on two facts—the elastic modu-

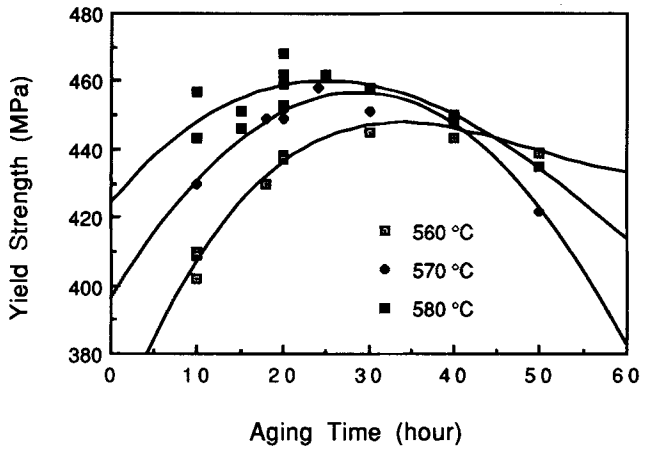

Fig. 5 Yield strength versus aging time at constant solution temperature.

lus was not dependent on heat treatment, and the ultimate strength and elongation data were slightly more random than the yield strength data. The randomness of the ultimate strength and elongation data is caused by the fracture process, which is much more random than the yielding of the material. For these reasons, the yield strength of the heat treated samples is the focus of the discussion below.

Figure 4 illustrates the relationship between yield strength and aging time for the solution temperatures examined. The trends that are present are typical of metals, which age to peak hardness and then overage. Overaging is caused by the agglomeration of precipitates, which decreases the average distance between precipitates. A metal reaches peak strength when the combination of precipitate size and distance is optimal. Because of the addition of reinforcements, the aging process of metal-matrix composites is not well understood. However, based on the results presented, metal-matrix composites age in a manner similar to metals.

One of the first groups of tests in the heat treatment study used a solution temperature of 530 °C, which is the standard T6 solution temperature for 6061 aluminum alloy. The samples heat treated to the T6 condition did not perform as well as reported by the manufacturer. The reported yield strength of SiC*p*/6061 aluminum aged for 18 hr was 414 MPa. As shown in Fig. 4, the experimental yield strength obtained after a 20-hr aging cycle was 317 MPa. After prolonged aging (>60 hr), the samples eventually approached the reported strength level of 414 MPa.

The discrepancy between the strength reported for SiC*p*/6061 aluminum in the T6 condition and that which was observed experimentally was largely unexplained. To account for this discrepancy, various factors were examined. If the material was manufactured in 1983, as was marked on the face of the composite sheet, the current mechanical properties reported by the manufacturer would not apply. In the early 1980s, the yield strength reported for 25 vol% SiC*p*/6061 aluminum was approximately 400 MPa.[13,14] However, the values observed experimentally were much lower. Because the heat treatment parameters used were well documented in previous studies and the furnace temperatures were varied, it is reasonable to assume that the lower strength observed for SiC*p*/6061 aluminum samples in the T6 condition was inherent to the composite sheet. Because the fabrication history of the composite sheet was unknown, further speculation is not possible. As will be discussed later, higher solution temperatures resulted in mechanical properties that were at or above the manufacturer's reported values.

Accelerated aging compared to the matrix alloy, as was reported for 7XXX and 2XXX SiC/aluminum composites in previous studies,[3,9,10] did not occur for the SiC*p*/6061 aluminum composite. The aging time for peak strength for 6061 aluminum sheet is 18 hr.[16] As shown in Fig. 4, aging of the composite compared to the matrix alloy was greatly decelerated. Even when the solution temperature was increased, the peak aging time never fell below 20 hr. To explain this discrepancy, the alloy composition of 6061 aluminum and those used in the previous studies were compared. The two 7XXX alloys were 6% Zn, 2.3% Mg, 1.8% Cu, bal Al[3] and 7% Zn, 2% Mg, 2% Cu, 0.14% Zr, bal Al.[10] The 2XXX alloy was 2204 aluminum[9] or 3.8 to 4.9% Cu, 0.3 to 0.9% Mn, 1.2 to 1.8% Mg, bal Al. The alloy used in this study was 6061 aluminum, or 0.8 to 1.2% Mg, 0.4 to 0.8% Si, 0.15 to 0.35% Cr, 0.15 to 0.4% Cu, bal Al. The increased aging times of the SiC*p*/6061 aluminum composites may have been due to the fact that Mg_2Si must precipitate from 6061 aluminum for hardening to occur. In the other alloys, zinc and copper compounds are the precipitates. The SiC particle may slow the precipitation of Mg_2Si in 6061 aluminum composites. As shown in Fig. 4, the aging time to peak strength decreased as solution temperature increased. Greater degrees of supersaturation of the matrix alloy probably accounted for this trend. With a higher potential for diffusion, precipitates were more likely to form with increasing supersaturation.

The yield strengths obtained during the heat treatment increased with solution temperature until a solution temperature of 590 °C was reached. At and above 590 °C, the strength values were erratic, as shown in Fig. 4. The lower bound of the melting temperature range of 6061 aluminum is 582 °C. Localized melting, resulting in matrix segregation, may account for the large scatter in the strength of the samples that were solution treated at temperatures above 580 °C.

In Fig. 5, the relationship between yield strength and aging time is presented for samples solution treated at 560, 570, and 580 °C. Second-degree polynomial approximations are included to represent the trends in the data. These three solution temperatures produced the best mechanical properties in the tested sample. From these data, the optimal heat treatment for SiC*p*/6061 aluminum was determined.

The maximum yield strength obtained was 462 MPa, which was the average value for samples heat treated at a solution temperature of 580 °C for 2 hr and aged for 20 hr at 160 °C. This value is a 12% increase over the reported yield strength of 414 MPa for the SiC*p*/6061 aluminum composite in the T6 condition.

At solution temperatures of 580 °C and above, the samples were slightly oxidized. The oxidation that occurred at 580 °C had little or no effect on the mechanical properties of the composites. Nevertheless, oxidation is undesirable. Attempts were

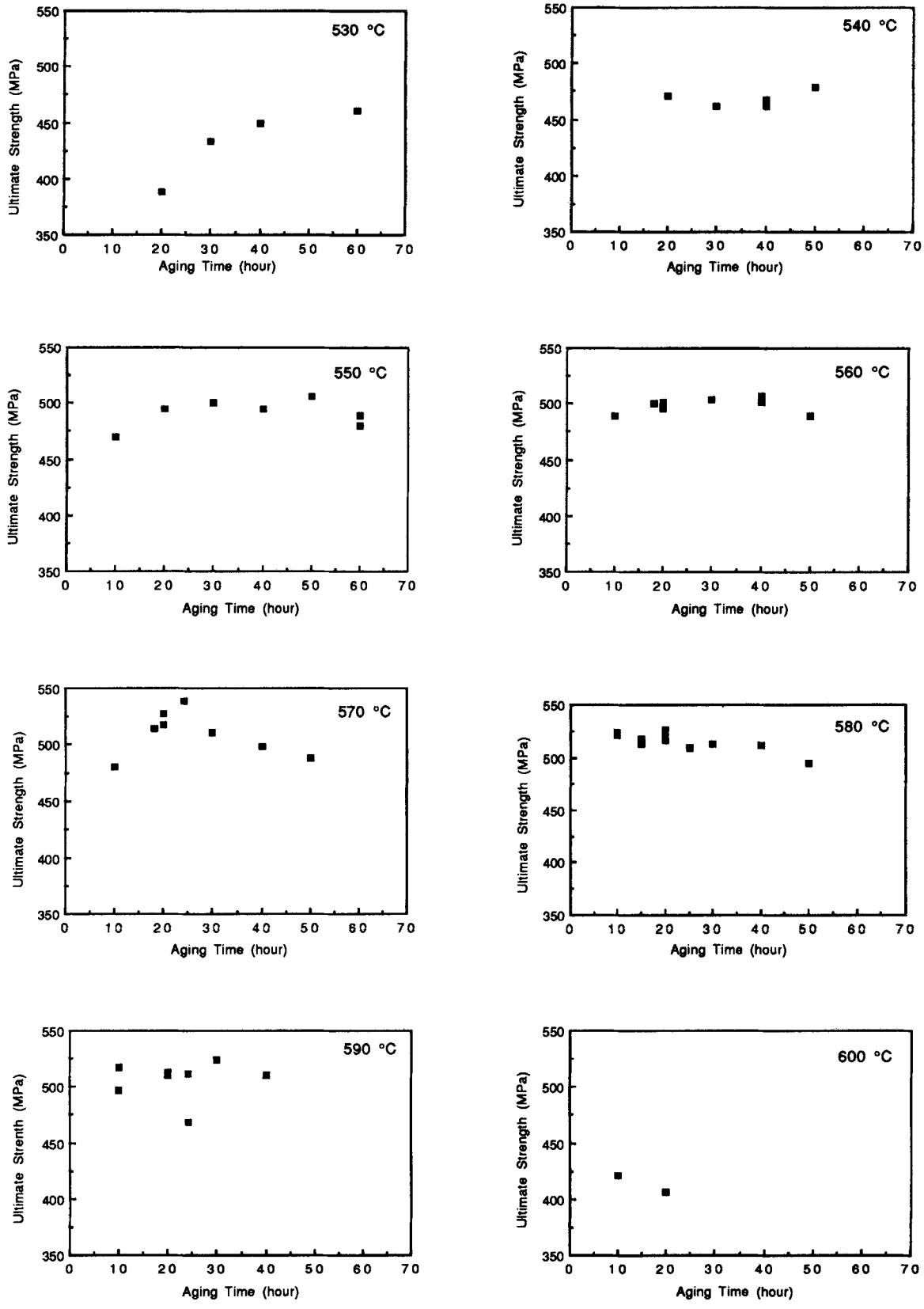

Fig. 6 Ultimate strength versus aging time (solution temperature 530 to 600 °C).

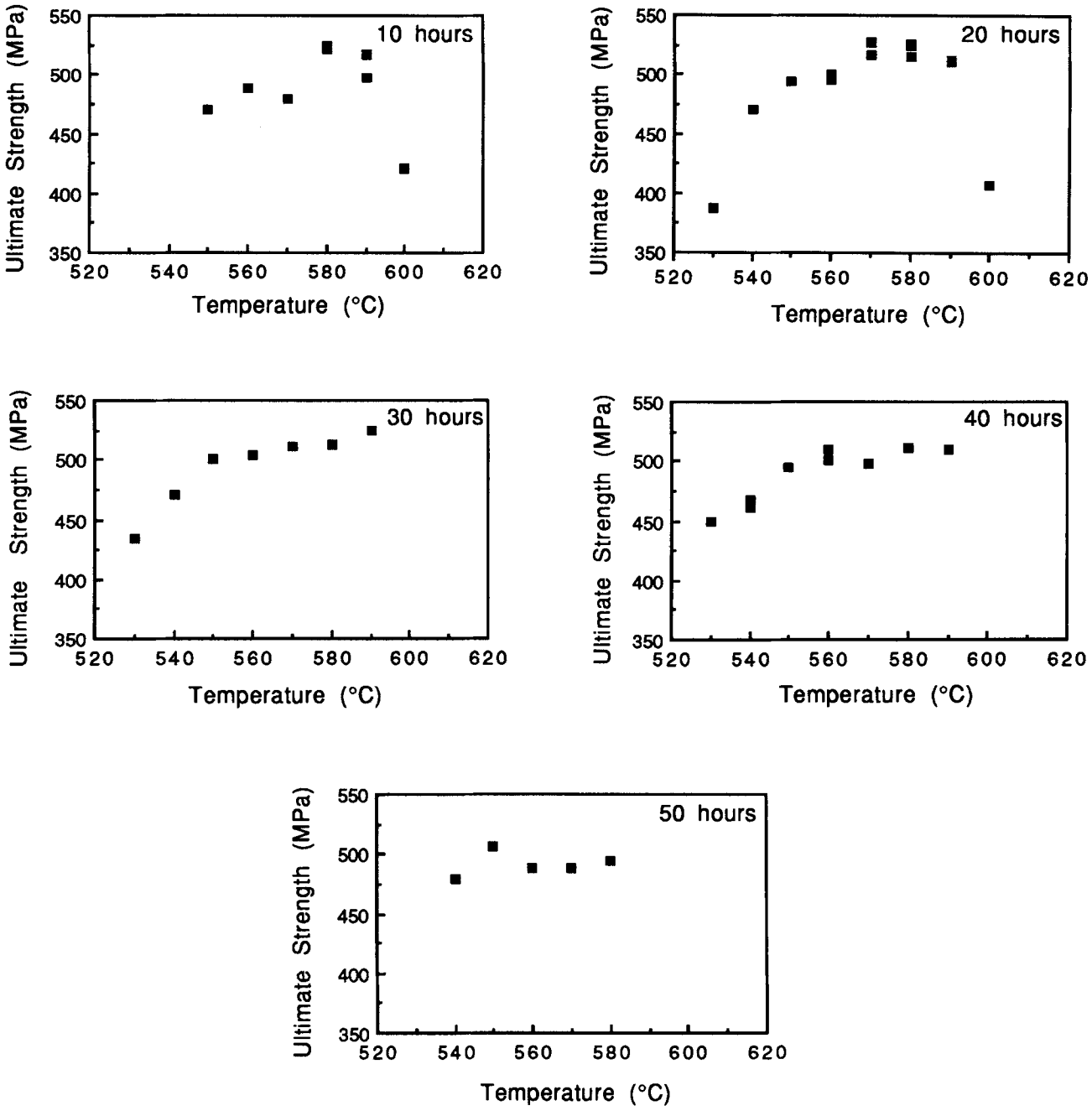

Fig. 7 Ultimate strength versus solution temperature (aging time 10 to 50 hr).

made to avoid this problem by solutionizing in a vacuum and an argon environment. When samples were solution treated in a vacuum, warping and severe degassing occurred. In an argon pressure of 1.2 atm and a solution temperature of 600 °C, the samples warped severely. Warping was most likely caused by the relatively high temperature and furnace configuration used during the controlled environment experiments. For these heat treatments, the specimens were placed in a fused quartz tube. However, no warping was observed in a sample solution treated at 600 °C in the box furnace. Therefore, the curved quartz surface probably caused the samples to warp. Low mechanical properties resulted from all of the controlled atmosphere experiments.

Rule-of-mixture equations for discontinuous fiber-reinforced composites are more appropriate for whisker composites, which have much higher aspect ratios than particle composites. By the rule-of-mixture, the predicted yield strength for SiC*p*/6061 aluminum is 290 MPa, whereas the pre-

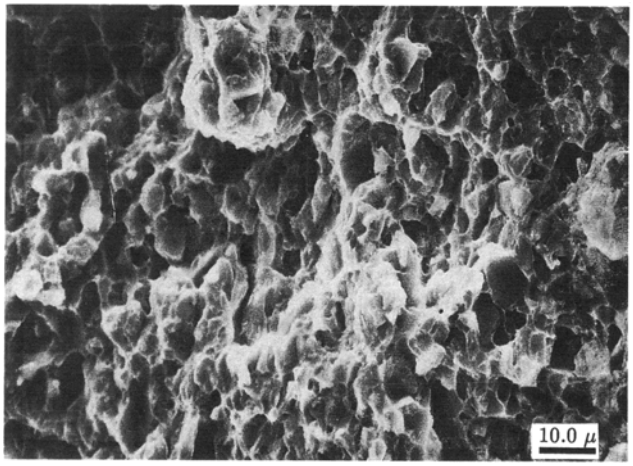

Fig. 8 SEM photograph of the fracture surface of the sample aged 40 hr (solution temperature 580 °C).

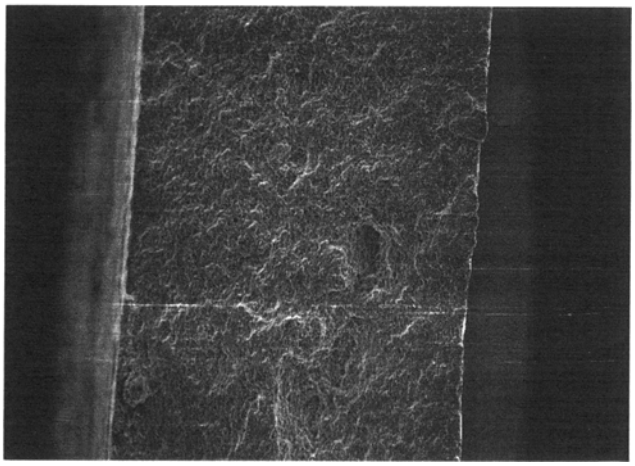

Fig. 10 SEM photograph of the fracture surface of the sample aged 40 hr (solution temperature 580 °C) showing cavities, raised areas, and ridges.

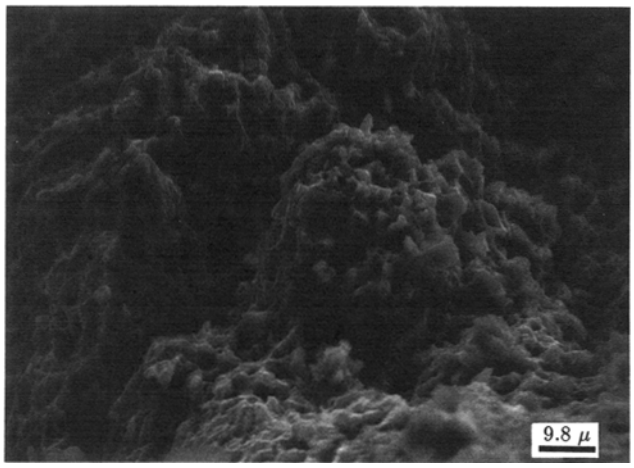

Fig. 9 SEM photograph of the fracture surface of a sample aged 20 hr (solution temperature 580 °C).

dicted ultimate strength is 318 MPa. The experimental values were 462 and 534 MPa, respectively. The rule-of-mixture equations assume that fiber pullout and matrix/fiber debonding are the dominant factors influencing composite strength. From SEM micrographs, which will be discussed later, this assumption is not applicable to heat treated SiC*p*/6061 aluminum, because the majority of the particles were fractured during tension tests. Therefore, the particles contribute more to the composite strength than is assumed in the rule-of-mixture.

Figure 6 shows the relationship between ultimate strength and aging time for all of the solution temperatures examined. Although slightly more random, the data presented in these graphs closely resemble the results for yield strength versus aging time presented in Fig. 4. Figure 7 shows the relationship between ultimate strength and solution temperature. These results resemble those of yield strength versus solution temperature. The randomness of the data can again be attributed to the nature of the fracture process in such composites.

Following the heat treatment study, SEM fractographic analysis was performed. Various fracture mechanisms of the SiC*p*/6061 aluminum composite were revealed. First, the fractured matrix consisted of small dimples, as is characteristic for ductile failure. However, macroscopic failure occurred in a brittle manner. It is known that ductile fracture is characterized by three stages—void initiation, growth, and coalescence. Because of the large volume fraction of SiC particles, that act as void initiation sites, the void growth and coalescence stages occurred very rapidly following void initiation. Therefore, a brittle macroscopic failure was observed. The dimples, or microvoids, ranged in size from 1 to 10 μm. Many microvoids were initiated at the second-phase (SiC) particles, as documented in a study by Nutt.[17]

Figures 8 and 9 show fracture surfaces of two samples. In the micrographs, the matrix appears dimpled, whereas the fractured particles are slightly darker and smoother. As shown in Fig. 8, the larger SiC particles fractured by cleavage, whereas the smaller particles caused microvoids and then either fractured or pulled out from the matrix. The larger cleaved particles ranged in size from approximately 3 to 8 μm, whereas the smaller particles found in the bottom of dimples were on the order of 1 to 3 μm. In Fig. 9, the same topography is present, except that the surface contains a raised area. This feature appears as a cavity, or fisheye, on the opposite fracture surface. Connected to the raised area are two channels that appear as ridges on the opposite fracture surface. These features suggest that some element on the tip of the raised area acted as a fracture initiation site, as documented in previous work.[2] The fracture initiator was probably located on the opposite fracture surface, at the center of a cavity.

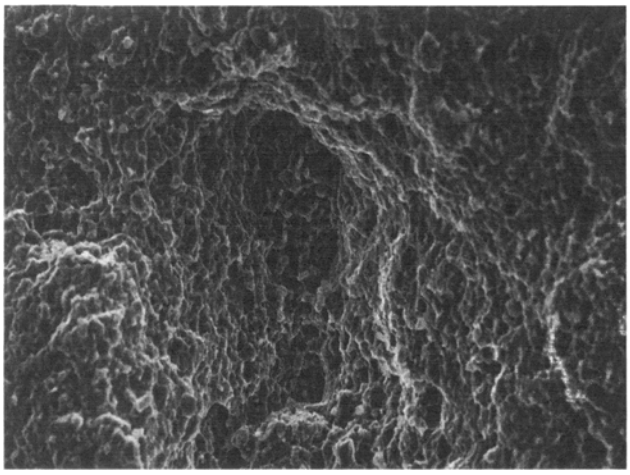

Fig. 11 SEM photograph of the fracture surface of the sample aged 40 hr (solution temperature 580 °C) showing a cavity or fisheye).

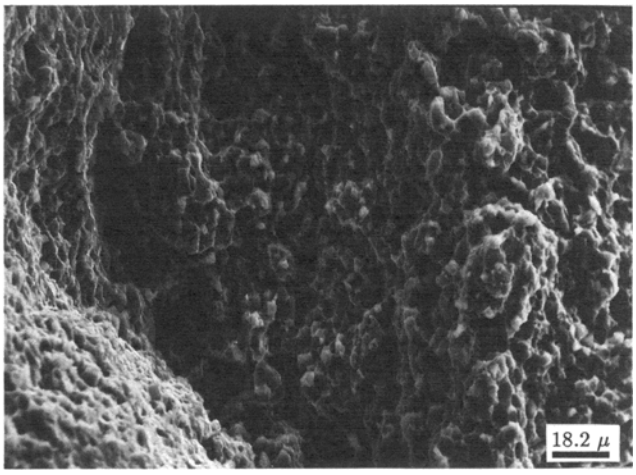

Fig. 13 SEM photograph of the fracture surface of the sample aged 30 hr (solution temperature 590 °C) showing a channel with large cleaved particles along its base.

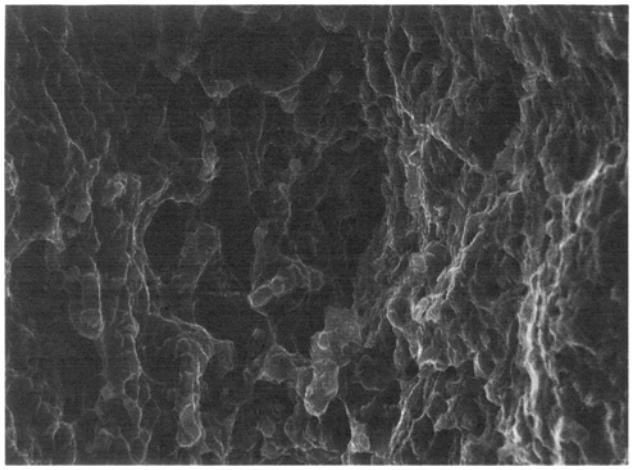

Fig. 12 SEM photograph of the fracture surface of the sample aged 40 hr (solution temperature 580 °C) showing the base of the fisheye containing many large cleaved particles.

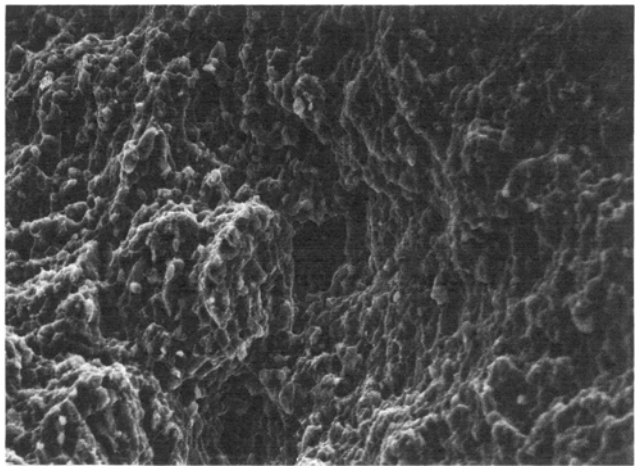

Fig. 14 SEM photograph of the fracture surface of the sample aged 20 hr (solution temperature 580 °C). A shallow cavity with an iron inclusion at its base is located at the center of the photograph.

Because the vast majority of the particles on the fracture surface were fractured, the full extent of the strengthening effect of the particles was used. In previous studies, reinforcement pullout has been more common than reinforcement fracture.[2,9,18] Because of the increased matrix strength due to the modified heat treatments, more load was transferred to the particles, resulting in particle fracture and higher composite strength.

Various fracture initiation sites were identified using SEM. Particle clusters acted as fracture initiation sites, as shown in previous studies.[2,8,10,18] In Fig. 10 through 12, a fisheye with a cluster of large particles at its base is presented. In Fig. 10, the fracture surface of the sample contains many cavities, raised areas, and ridges. Figure 11 shows a closeup of the largest cavity. At the base of the cavity, many large cleaved particles are present, as shown in Fig. 12.

Channels were also caused by particle clusters. In Fig. 13, a channel is pictured with large cleaved particles at its base. In addition, many small particles at the bases of dimples are present in this micrograph. Large particles contribute greatly to the strength of the material, as is evidenced by the degree of large particle fracture on the fracture surface. However, a reduction in the degree of clustering of the large particles would be beneficial to composite strength.

Another type of fracture initiation site was documented during SEM analysis. Inclusions containing large percentages of

iron were observed in some cavities and along cracks in the composite. In Fig. 14, an iron-rich inclusion is shown at the base of a shallow cavity. The inclusion appears darker than the surrounding matrix and particles because of its iron content.

The iron inclusions were detrimental to the composite strength, as is evident by their location at the bases of cavities and along cracks. However, the origin of these inclusions remains unknown. Because they were found well within the matrix, they were probably introduced during fabrication, perhaps as debris from the extrusion or rolling machinery. Numerous iron inclusions were found. Their presence may be part of the reason that the T6 heat treatment strength did not match the manufacturer's reported values.

In summary, the modified heat treatments resulted in significantly increased mechanical properties of SiC*p*/6061 aluminum. Particle clusters, large particles, and iron inclusions acted as fracture initiation sites. Measures taken to avoid these defects during composite manufacturing would further increase the mechanical properties of SiC*p*/6061 aluminum.

4. Conclusions

The strength of SiC*p*/6061 aluminum is greatly dependent on heat treatment. The trends that occur during heat treatment of SiC*p*/6061 aluminum are similar to those that occur during heat treatment of aluminum alloys. However, to obtain optimal matrix properties, the effect of the presence of SiC particles must be countered by varying heat treatment parameters.

For SiC*p*/6061 aluminum, significant increases in strength are possible by modification of the standard T6 heat treatment for 6061 aluminum. In particular, increasing the solution temperature results in increased composite strengths. Yield strength increases up to 12% were observed for SiC*p*/6061 aluminum compared to the reported values for the T6 condition. Both particle clusters and iron-rich inclusions act as fracture initiation sites in SiC*p*/6061 aluminum.

References

1. R. DeMeis, *Aerospace American*, Mar 1989, p 26.
2. B.J. Maclean and M.S. Misra, Proc. *Symp. Mechanical Behavior of Metal Matrix Composites*, Dallas, Feb 1982, J.E. Hack and M.F. Amateau, Ed., The Metallurgical Society of AIME, 1983, p 301.
3. C.G. Krishnadas Nair, M.R. Krishvadev, and D. Dutta, *32nd Int. SAMPE Symp. Exhibition*, Anaheim, Apr 1987, R. Carson *et al.*, Ed., Vol 32, Society for the Advancement of Material and Process Engineering, 1987, p 889.
4. P. Niskanen and W.R. Mohn, *Adv. Mater. Proc.*, July 1987, p 41.
5. E.J. Kubel, *Mater. Eng.*, Vol 100 (No. 3), 1984, p 47.
6. L.J. Fu, M. Schmerling, and H.L. Marcus, *Composite Materials: Fatigue and Fracture, A symposium on High Modulus Fibers and Their Composites*, Dallas, Oct 1984, H.T. Hahn, Ed., ASTM, 1984, p 51.
7. S.V. Nair, J.K. Tien, and R.C. Bates, *Int. Met. Rev.*, Vol 30 (No. 6), 1985, p 275.
8. D.F. Hasson, S.M. Hoover, and C.R. Crowe, *J. Mater. Sci.*, Vol 20, 1985, p 4147.
9. M.D. Skibo, "Stiffness and Strength of SiC-Al Composites," SAND81-8212, Sandia National Laboratories, Livermore, June, 1981.
10. J.J. Lewandowski, C. Liu, and W.H. Hunt, Jr., *Symp. Interfacial Phenomena in Composites: Processing, Characterization, and Mechanical Propeties*, Newport, 1988.
11. J. England and I.W. Hall, *Scripta Metall.*, Vol 20, 1886, p 697.
12. ASTM Standard D 3552-77,1988.
13. W.C. Harrigan, Jr., G. Gaebler, E. Davis, and E.J. Levin, *Proc. Symp. Mechanical Behavior of Metal Matrix Composites*, Dallas, Feb 1982, J.E. Hack and M.F. Amateau, Ed., The Metallurgical Society of AIME, 1983, p 169.
14. W.A. Logsdon and P.K. Liaw, *Eng. Fract. Mech.*, Vol 24 (No. 5), 1986, p 737.
15. D. Webster, "Properties and Microstructure of Metal Matrix Composites," 5-8404, Wright-Patterson Air Force Base, Ohio.
16. *Handbook of Aluminum*, Aluminum Company of Canada, Ltd., Montreal, 1970.
17. S.R. Nutt, *Proc. Symp. Interfaces in Metal-Matrix Composites*, New Orleans, Mar 1986, A.K. Dhingra and S.G. Fishman, Ed., The Metallurgical Society of AIME, 1986, p 157.
18. D.L. Hunn, *Proc. Symp. Mechanical Behavior of Metal Matrix Composites*, Dallas, Feb 1982, J.E. Hack and M.F. Amateau, Ed., The Metallurgical Society of AIME, 1983, p 83.